Performance Improvement of Duty-Cycle Division Multiplexing System Utilizing Symbol Coding Customization

M. N. DERAHMAN[1], A. MALEKMOHAMMADI[2], G. GNANAGURUNATHAN[2], M. K. ABDULLAH[3], K. DIMYATI[4], K. A. NOORDIN[4]
[1]Department of Communication Technology and Networking, University Putra Malaysia, Malaysia
Department of Electrical and Electronic Engineering, The University of Nottingham, Malaysia
Research and Development Department, Significant Technologies, Sdn, Bhd, Malaysia
[1]Department of Electrical Engineering, Faculty of Engineering, University of Malaya, Malaysia
mnoord@upm.edu.my, aminmalek_m@ieee.org

Abstract: -This paper looks at the novel method employed to improve the performance of the Duty-Cycle Division Multiplexing (DCDM) system. The proposed method involves signal processing and customisation of the signal at the transmitter side. This technique regulates the amplitude level of existing waveform into different levels in such a way that the appropriate eye-height is increased. The regulation is made possible based on the feedback received according to the condition of the received signal sent previously. This novel method enables a 7 dB improvement in comparison to the conventional model. In addition to that, performance for all transmitted channels is maintained in contrary to previous research outcomes.

Key-Words: - Optical communication, Multiplexing, Signal processing, Duty cycle Division Multiplexing

1 Introduction

There is a plethora of multiplexing techniques that have been developed for the purpose of augmenting the transmission capacity or bandwidth in fiber optic transmissions. Conventionally, most of such techniques are based on time, frequency and/or wavelength domains namely Time Division Multiplexing (TDM) [1, 2], Frequency Division Multiplexing (FDM) [3] and Wavelength Division Multiplexing (WDM) [2, 4]. TDM for example, divides the time into several recurrent time slots of certain duration to accommodate a fixed number of sub-channels. Each user is given a specific time slot in order to transmit. Thus, the full transmission ability of high capacity transmission medium can be utilized by multiplexing several users' data in the time domain. However, this capacity can be further increased by introducing a new multiplexing technique namely Duty-cycle Division Multiplexing (DCDM). The DCDM, first introduced by [5] proposes the idea of utilising different RZ's duty-cycle for each user. Different user signal waveforms are multiplexed in a channel within the same time period and at the same wavelength (or frequency). In this case, the signals are encoded from multiple users' data with different properties of duty-cycle and power level (amplitude). Therefore, DCDM is a multiplexing technique, which serves the dual function of data encoding and combining the sub-channels during transmission.

Thence, the transmission of multiple users' data over a sub-channel in a medium can be materialized through capitalizing both the time and wavelength domains, which in turn increases the total channel capacity.

In [5], simultaneously transmitting data over DCDM waveforms outperform other modulation scheme namely TDM [5, 6]. However, one disadvantage of an early DCDM technique is that the performance of various channels is not uniform [7]. For instance, at a BER of 10^{-9}, the receiver's sensitivity is recorded to be at -23 dB, -26.5 dB and -30 dB for User 1 (U1), User 2 (U2) and User 3 (U3), respectively. The discrepancy is particularly obvious between U1 and U3. This situation will introduce difficulties in an environment where a common transmission standard is required. For example, it is costly to characterize and define the transmission capability due to the requirements of different receiver's sensitivities. Furthermore, intelligent receivers are required to differentiate the incoming waveform/signal from each channel.

Thus, the focus of this paper is (a) to improve the performance of DCDM and (b) to reduce the performance discrepancies between the multiplex channels. This is achieved through customisation of the amplitude levels of the DCDM symbols at the transmitter side based on the feedback received according to the condition of the received signal sent earlier.

This approach is able to cushion the impairments due to noise and dispersion, which directly influences the BER.

The outline of this paper is as follow: at the outset, brief history about DCDM including the working principles and an explanation of the DCDM simulation setup are involved. The power levels function associated with the eye-opening are also elaborated here. Following this, the eye-opening of the DCDM signal in relation to the performance of each user is discussed in the subsequent section. In order to substantiate the proposed method, the simulated results are reported and discussed in the subsequent section.

2 DCDM WORKING PRINCIPLE AND THE SIMULATION SETUP

Fig. 1 shows the block diagram of the simulation setup of the Duty-Cycle Division Multiplexing (DCDM) system. It comprises three main components namely transmitter, communication medium and the receiver. The transmitters are generating data at PRBS of 2^{23} -1 at 10 Gb/s (per channel). The incoming user's data are fed and converted from non-return to zero (NRZ) to return to zero (RZ).

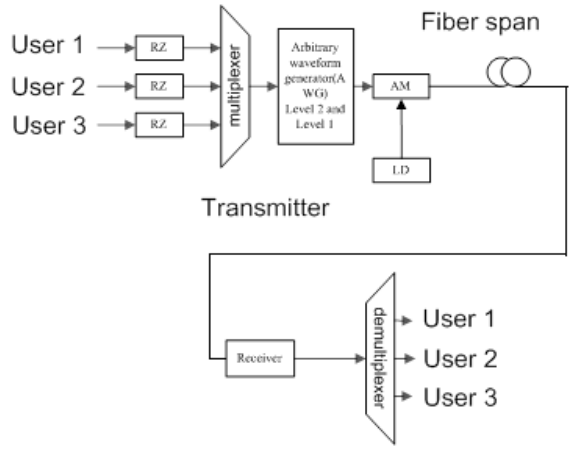

Fig. 1: The simulation setup for DCDM system (10 Gbit/s per channel)

The pulse shape used in the analysis is Gaussian, representing the RZ format, which can be described by [8].

$$E(t)=\begin{cases}1-e^{-(t/cr)^2} & 0\le t<t1\\ 1 & t1\le t<t2\\ e^{-(t/cf)^2} & t2\le t<tc\\ 0 & tc\le t<ts\end{cases} \quad (1)$$

where *cr* and *cf* are the rise time and fall time coefficient, respectively. The *t1* and *t2*, together with *cr* and *cf* are numerically determined so that pulses with the exact values of the rise time and fall time will be generated. *tc* is the duty cycle value, which represents the duration of high level within a bit period, and *ts* is the bit period. All users' data are multiplexed using a power combiner (electrical adder) resulting in a DCDM signal. The DCDM symbol mimicking "stair case" is established. For instance, if U1, U2 and U3, are carrying bit '0's, the DCDM waveform pattern can be seen in Case 1 in Fig. 2. Meanwhile, bit period (Ts) of each waveform is associated with four slots (Slot1–Slot4). The number of slots is associated with the number of incoming users following (n+1) rule, where "n" is the number of users. These slots are due to the RZ duty-cycles of original users' symbol duration. Meanwhile the combination of the original user's signal amplitude level contributes to the amplitude of the waveform.

As shown in Fig. 2(d) the generated DCDM signal has specific patterns. These symbol patterns are characterized by different duty-cycle and power level associated with each user.

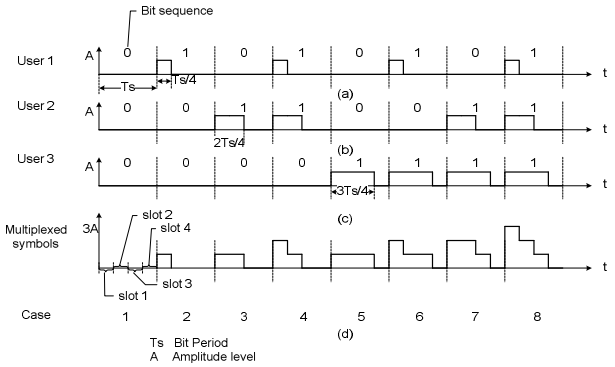

Fig. 2: (a) Possible DCDM pattern for U1. (b) Possible pattern for U2. (c) Possible pattern for U3. (d) Multiplexed signal for U1, U2 and U3.

The DCDM data is then modulated through constant wave (CW) laser diode at 1550 nm wavelength. Using an external modulator; the optical field at the output of the optical modulator is given by [9].

$$E_{out}(t) = E_{in}(t).\cos(\Delta\theta(t)).\exp(j.\Delta\varphi(t)) \quad (2)$$

where $E_{in}(t)$ is the optical field at the input of the MZM, $\Delta\Theta$ is the phase difference between the two waveguide branches in MZM and $\Delta\Phi$ is the signal phase change defined as :

$$\Delta\varphi = SC \times \Delta\theta(t) \times (1+SF)/(1-SF) \quad (3)$$

In Equation (3), the parameter *SC* is ±1 if negative signal chirp is disabled or enabled, respectively, and *SF* is the symmetry factor.
The fiber is modelled using a low pass equivalent representation of a linear bandpass system in which the fiber dispersion is accounted through the quadratic (nonlinear) phase response of the fibers transfer function, given by [8]

$$H_{fib}(f) = \exp\left(j\frac{\Pi DL\lambda^2 f^2}{c} - (\alpha.L/2) \right) \quad (4)$$

where, λ is the operating wave length (1550 nm), c is the free-space speed of light, *D*=17 ps/(km.nm) is the fiber's linear dispersion coefficient, *L* is the fiber length, and α is the attenuation coefficient. Next we assume an EDFA gain, equal to *G* at the operating wavelength and amplified spontaneous emission (ASE), n_{sp}The optical power *P (t)* is then given by [8].

$$P(t) = 2\sqrt{G c_1 c_2}\, s(t)[n_c(t)\cos\varphi_s(t) + n_s(t)\sin\varphi_s(t)] + G c_1 c_2 s^2(t) + c_2[n_c^2(t) + n_s^2(t)] \quad (5)$$

where the coefficients *c1* and *c2* are the input and output coupling losses of the optical pre-amplifier, respectively and *s(t)* is the received amplitude of the optical field at the receiver. The noise process is described by two zero mean Gaussian distributed random variables, $n_c(t)$ and $n_s(t)$, corresponding to the in-phase and out-of-phase noise components of the band limited noise process, respectively. The power spectral density of the ASE noise, per polarization, is given by [8-9]

$$N_{ASE} = (G-1)hv\, n_{sp} \quad (6)$$

where hv is the photon energy. The variance (power) of the random variables is therefore

$$\sigma^2 = P_{ASE} = (G-1)hv\, n_{sp} B_0 \quad (7)$$

where B_0 is the noise equivalent bandwidth of the optical filter.
At the receiver side, the optical signal is detected by a photodiode and passed through a low-pass filter (LPF) and Clock-and-Data-Recovery (CDR) unit.
The photodetection is incorporated in to the model as a Poisson process with intensity

$$\lambda(t) = \frac{\eta}{hv} P(t) + \lambda_0 \quad (8)$$

where η is the quantum efficiency of the power conversion process and λ_0 is the dark current. From (8), the mean (9) and variance (10) of the detection current are derived

$$E[I_d] = R_s G c_1 c_2 s^2(t) * h_e(t) + 2 c_2 P_{ASE} R_s H_e(0) + q\lambda_0 H_e(0) \quad (9)$$

$$\sigma_{I_d}^2 = q R_s c_1 c_2 s^2(t) * h_e^2(t) + 2q R_s c_2 P_{ASE} B_e + 4 R_s^2 G c_1 c_2^2 N_{ASE} \times \int \left| \tilde{r}(f).H_o(f) * H_e^*(f)\, e^{-j2\Pi ft}.H_o(f) \right|^2 df + q^2\lambda_0 B_e + 2R_s^2 c_2^2 N_{ASE}^2 I_2 \quad (10)$$

where R_s is the responsivity of the photodiode which is equal to $q\eta/hv$, where *q* is the electron charge, $h_e(t)$ and $H_e(0)$ are the impulse response and the DC gain of the electrical filter, respectively. In (11), B_e is a measure of the noise equivalent bandwidth of the electrical filter.

$$B_e = \int_{-\infty}^{\infty} |H_e(f)|^2 df \quad (11)$$

The noise bandwidth of the ASE-ASE beat noise is measured through I2, which is calculated by [11]

$$I_2 = \int_{-\infty}^{\infty} |H_e(f)|^2 |H_o(f)|^2 * |H_o(f)|^2 df \quad (12)$$

where $H_e(f)$ and $H_o(f)$ are transfer functions of the electrical and optical filter, respectively. The contribution from the thermal noise was also added as an additional term in (10).
After the signal passes through the transmission medium and reaches the receiver end, the signal detection and bit regeneration takes place. In order to decide on the incoming signal, the inference rules are used as shown in Table I. The decision is based on the fixed threshold values, which is assigned into

three different values associated with each level (th1, th2 and th3). To describe this, consider Case 1 in Fig. 2 (d). In this example, the received signal amplitude is less than th1, which refers to the first rule in Table I, the receiver (R1) is assumed to receive a bit 0.

Table I: The Decision Making Rules

No	User	Rule	Decision	Case
1	U1	if (S1 < th1)&(S2 < th1)	then U25=0	1
2	U1	if (th3 ≤ S1 < th2)&(th15≤ S2 < th4)	then U25=0	3, 5
3	U1	if (th2 ≤ S1 < th1)&(S2 ≥ th4)	then U25=0	7
4	U1	if (th3 ≤ S1 < th2)&(S2 < th5)	then U25=1	2
5	U1	if (th2 ≤ S1 < th1)&(th5 ≤ S2 < th4)	then U25=1	4, 6
6	U1	if (S1 ≥ th1)&(S2 ≥ th4)	then U25=1	8
7	U2	if (S2 < th5)&(S3 < th6)	then U50=0	1, 2
8	U2	if (th5 ≤ S2 < th4)&(S3 ≥ th6)	then U50=0	5, 6
9	U2	if (th5 ≤ S2 < th4)&(S3 < th6)	then 50=1	3, 4
10	U2	if (S2 ≥ th4)&(S3 ≥ th6)	then U50=1	7, 8
11	U3	if (S3 < th6)	then U75=0	1, 2, 3, 4
12	U3	if (S3 ≥ th6)	then U75=1	5, 6, 7, 8

Note that the DCDM simulation setup includes an Arbitrary Waveform Generator (AWG) [11] before the Match-Zehnder Modulator (MZM). The function of the AWG in this case is to modify the transmitted power level according to the eye-opening requirements (the working principle of AWG will be elaborated in depth henceforth). The implementation of AWGN makes it different from [10] thereby enabling power level regulation. The power level of transmitted waveform can be regulated at several stages or levels according to BER requirements at the receiver. These modified signals are then transmitted through 80 km single mode fiber (SMF). The dispersion effect is negligible due to the use of dispersion compensation fiber (DCF).

The main function of AWG is to set the transmitted amplitude for each level. In doing so, a mapping function is used (see Table II). It can be implemented as a simple algorithm embedded in the AWG. Its function is to combine the source bit sequence (three bits) of the individual users and transform them into a DCDM signal. This signal or symbol can be customised as required so as to increase the vertical eye opening. For example, consider that a '111' user's bits combination, the original amplitude levels (3, 2, 1) will produce an eye-pattern as shown in Fig. 3. In order to increase the eye-1 of Fig. 3(a), the amplitude level 2 needs to be decreased (in this case, the amplitude level 3 cannot be increased since the maximum power level is 1). With that approach, one can increase the height of eye-opening of eye-1 as in Fig. 3(b). In the perspective of DCDM level, the original level of Level 2, which is taking the value of 2, can be attuned to 1.8. Indirectly, this will increase the eye-1 high. However, the effect of this technique is set to reduce the eyes relates to the neighbouring levels (eye-2 and eye-3). This effect cannot be avoided due to the limited signal space with regard to the power set.

As the symbol reaches the receiver, the direct detection method is used to convert the DCDM signal into the electrical signal. The signal is then recovered based on the setting threshold level by a decoder circuit as implemented in on-off keying systems [9]. In order to decide on a single bit, the rules based on decision-making are considered [8,10] as multiple slots and levels are involved. For instance, S1 and S2 are used to decide on the bit sequence for U1 whereas S2 and S3 are used for U2 and Slot 3 (S3) for U3.

This simulation setup is slightly different from that of [7] in terms of level spacing mechanism and the AWG implementation. In [5], a specific coefficient function is used to regulate the power level 1 and power level 2 with the same coefficient rate (see Fig. 3). Apart from that, the approach used in this research allows separate spacing values between two levels without the need to follow a specific coefficient value. Thus, the eyes in each associated levels can be further attuned to achieve a better BER with customised spacing criteria. The spacing value can be set by running customisation algorithm, on the AWG through a feedback channel [11-13] and by setting the associate amplitude at various levels. This implementation, mimicking [14], is where an

adaptive transmitter is used to change its modulation format to/from BPSK, QPSK and QAM. The feedback channel in this case utilizes general-purpose interface bus (GPIB) to send the amplitude and phase requirement to the transmitter. The same out-of band channel feedback is used in [12]. A state generator is located just before the receiver and is used to monitor the active channel and send the feedback state to the transmitter.

Table II: Bit-to-signal Mapping Function

Bits combination from U1, U2 and U3	**Original level per slot (Slot 1, Slot2 and Slot 3)**	**New amplitude level (Slot 1, Slot2 and Slot 3)**
000	0, 0, 0	0, 0, 0
001	0, 0, 1	0, 0, 1
010	1, 1, 0	1, 1, 0
011	2, 2, 1	2, 1.8, 1
100	1, 0, 0	1, 0, 0
101	2, 1, 1	2, 1, 1
110	2, 2, 0	2, 1.8, 0
111	3, 2, 1	3, 1.8, 1

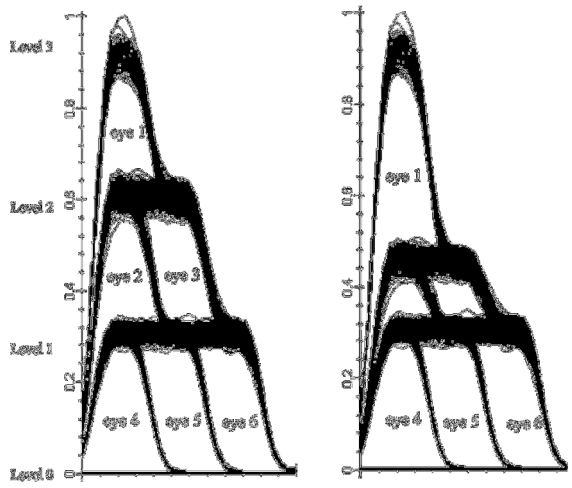

Fig. 3: (a) original eye-opening. (b) eye-high for eye-1 is increased

3 BER CALCULATION

Bit error rate (BER) is basically the ratio between eroded received bits over total received bits. This is the best method to calculate the BER, but it is limited and time-consuming as the long span system is currently being investigated [15]. Instead, the probability method based on Q value is used in this study to evaluate the performance [5, 6]. The assumption of Gaussian noise on bits '0's and '1's in relation with its mean value and the standard deviation for each level are used in this study. The quantity, Q is given by:

$$Q_i = \frac{\mu_1 - \mu_0}{\sigma_1 + \sigma_0} \tag{13}$$

where μ and σ are the means and the standard deviations for each of the eyes, respectively. The BER can be calculated based on (13) and is given by

$$BER_i = \frac{1}{2}\, erfc\left(\frac{Q_i}{\sqrt{2}}\right) \tag{14}$$

The basis of BER calculation in DCDM is based on Fig. 3, and it is associated with the respective received eyes in Fig. 4. The probability of errors (Pe) of each eye can be associated with Pe's of the respective eye. For instance, at eye-6 (Fig. 3), the Pe is associated with PeI and PeH of Fig. 4. Thus, the Pe at eye-6 is best described by

Pe(eye-6) = ½ *(PeH+PeI); (15)

where PeH is the probability of error being '0' and PeI is the probability of errors of being '1'. Both are error probabilities at eye-6 based on its threshold value of th6.

As stated in Table I, the data recovery and BER calculation for U3 is only related with rules 11 and 12 where it can be described as

if (S3 <th6) then U3 = '1' else if (S3 ≥ th6) then U3 = '1' (16)

thus, the error probability for U3 is described as

BERU3 = Pe(eye-6) (17)

Based on the combination of these simple rules and the associated *Pe* of each eye, the BER for individual users can be summarized as follows:

BER U1 = ½ *((PeA + PeBm*PeFs + PeCm*PeG) + (PeBs*PeE + PeCs*PeFm + PeD)) (18)

BER U2 = ½ *((PeE + PeFm*PeI) + (PeFs*PeH + PeG)); (19)

BER U3 = ½ *(PeH+PeI); (20)

For BER of U1, several Pe involves; PeA is the error probability associated with eye-1.

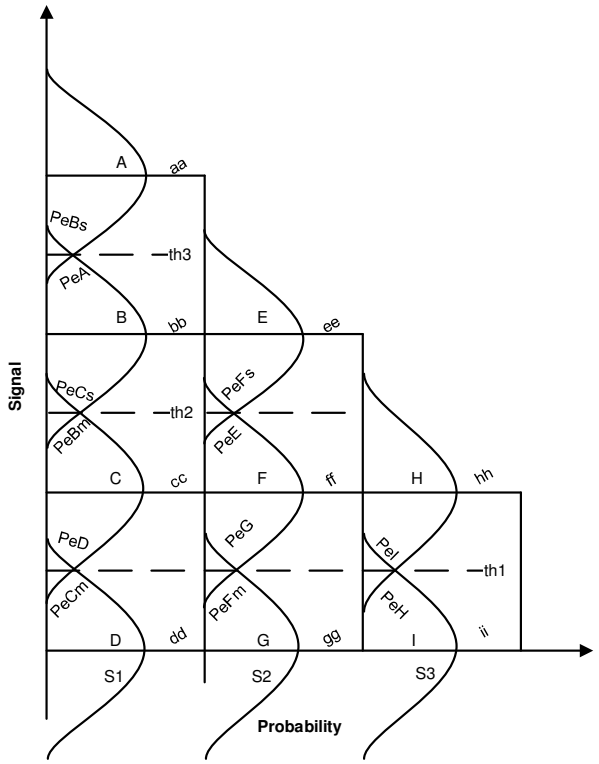

Fig. 4: probability of errors

The *PeA* comes into picture when the amplitude level is beyond level-3. The next Pe's parameters are *PeBm* and *PeFs*. These two parameters are associated with level-2 but in between two adjacent slots (S1 and S2). It is logic to assume that (see Table I) to determine the bit sequence, two slots will be examined. In this case, the error is to be compensated by each other's slot. Thus, in the mathematical formula, multiplying the Pe of S2 at the same level can reduce the Pe in S1. The error can be reduced if the both Pe values are less than 1. Since, *PeA* and *PeD* do not have its pair to compensate; it is significant to decrease this value. *PeA* was chosen owing to the ease in enlarging the eye-1 with less effect to the other slots as compared with *PeD*.

The calculation of Pes is based on the received eye patterns. This is solely dependents on the size of the eye. The larger the vertical eye-opening the more noise tolerated at the receiver side [15, 16].

In this case, each *Pe* is associated with different user's BER. Thus, it is important to choose which Pe and eyes are involved with the target user's BER. By regulating the power level at transmitter, it is believed that impairments such as noise will be cushioned.

From this point of view increasing the transmitted power level leads to eye-high increments at the receiver side, which consequently can reduce the BER. Not that the higher the level of signal amplitude the lower the probability of the error. As an example, at eye-6 (in Fig. 3), by increasing the amplitude of the level 1, the value of *PeH* and *PeI* will reduce accordingly, which leads to better performance for U3.

Note that the main aim is to optimize the level distribution between different eyes while the maximum amplitude is fixed.

4 Results and Discussion

In the first stage, the simulations were conducted to optimize the eye-opening of specific eye while the maximum voltage level is fixed. Eye-1 was chosen since its probability of error (Pe) was high. Furthermore, *Pe* for eye-1 solely contributed to BER calculation of U1, as it could not be compensated by another *Pe* from other slots. Nevertheless, *PeD* was quite low due to the larger eye-opening of eye-4 as discussed above and shown in Fig. 3(a).

Fig. 5 shows an improvement of more than 1dB at the BER of 10^{-9} as compared to the previous result reported in [6] for the U1. This was achieved by increasing the high-opening of eye-1 to 120%. Further improvement of 2dB could be obtained when the eye height reached 130%. It was actually due to the significant reduction of the probability of error of eye-1, *PeA*. As the opening of Eye-1 increased towards 140%, it gave a negative impact to the BER. This was due to the limitation of an amplitude level in DCDM waveform where all users had to share the same signal space.

Note that as shown in Fig.3 (b) in order to maintain the maximum amplitude level, increasing the eye high in eye 1 automatically results in reducing the eye high for eye 2, which, in turn will affect the performance of U2. Therefore based on the simulation results, shown in Fig. 6, in order to maintain the acceptable performance for U2, the eye high for eye1 can be increased by maximum of 120%. As shown in Fig. 7, channel 3 (U3) still outperforms as compared to U2 and U1. By this optimization, the performance of channel 1 and 2 are closed to each other but still there is a huge gap between the performance of these two channels and channel 3.

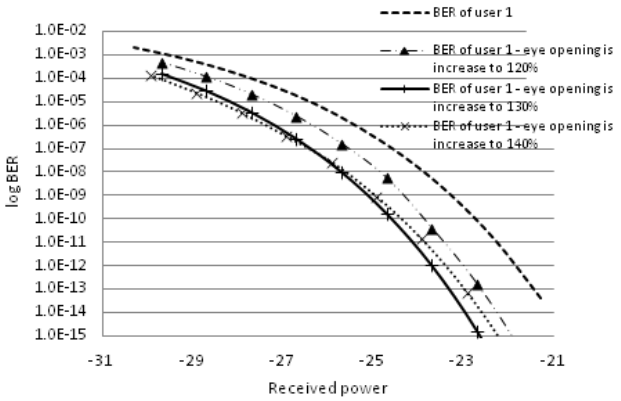

Fig. 5: The effect of varying level 2 on the receiver sensitivity of channel 1

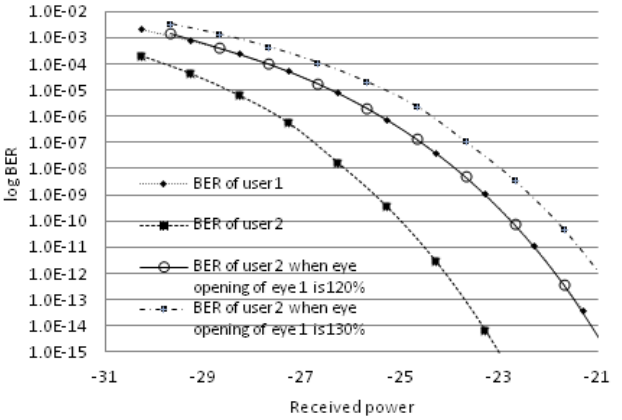

Fig. 6: The effect of increasing eye-height of eye-1 to the performance of U2

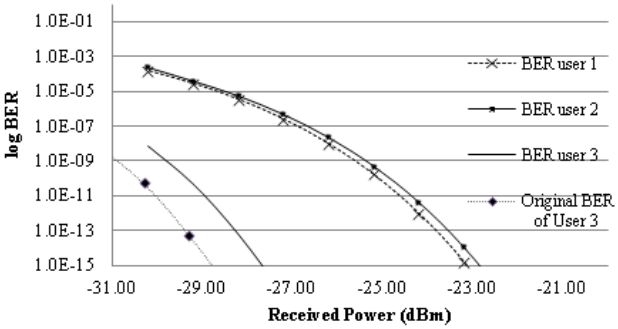

Fig. 7: Performance comparison between all three channels after the optimization

In order to decrease the gap between the performances of all three channels, the amplitude of level 2 is adjusted to 1.4 whilst Level 1 is set to 0.42 (instead of 1). Thus, the gap between Level 3 and Level 2 is increased to 160% whilst the gap between Level 2 and Level 1 is slightly decreased to 98%. As a result of this adjustment, the gap between Level 1 and Level 0 is reduced to only 42%. It shows that the receiver sensitivity at this point increased to 7 dBm (at the BER of 10^{-9}). Note that this optimization affects the sensitivity of U3 as it degrades by 2 dB, but it is still within the acceptable BER of 10^{-9}. As shown in Fig. 8 and as opposed to the previously reported work [5], these optimizations, leads to almost same performance for all three channels.

With this so-called optimum power setting level, the calculation is extended using different fiber length and dispersion levels. For the first scenario, the SMF fiber length is varied ranging from 20-110 km. The amplifier is then set before the receiver with noise figure (NF) of 5 dB and a gain of 30 dB. The plotted results for the SNR over fiber length can be seen in Fig. 9. As expected, the SNR for the amplified signal is higher as compared to the non-amplified one. It is particularly obvious when the fiber is less than 70 km. However, as for both cases, the customised transmitted power level leads to 2 dB improvements in terms of SNR.

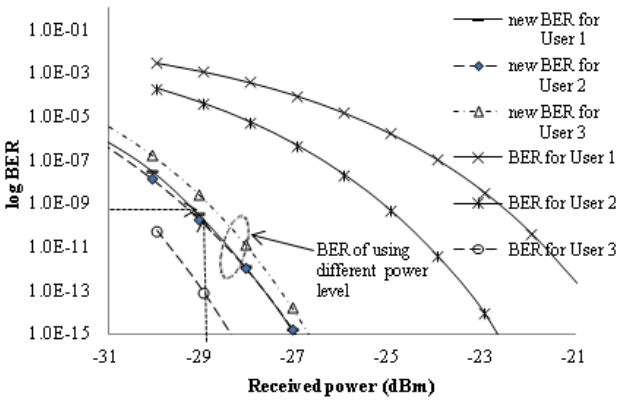

Fig. 8: performance comparison between the conventional channels (BER of U1, 2 and 3) and the optimized channels (new BER for U1, 2 and 3

Meanwhile, in the perspective of the fiber span, the non-customised level is out performed for the fiber length less than 84 km. In the normal circumstances, the BER performances will follow the SNR. In this case, the customised level will improve the performance by reducing the BER. However, it is not exactly the case in DCDM as its decision, dependents on more than one slot. Furthermore, the SNR actually decreases when the transmitted power level is mitigated. However, with reference to Fig. 5, the simulation results show that with an extension offered in the decision rules, the performance of the system improved greatly. This proves that by referring to other slots, the decision-making is more accurate owing to the negation of noise effects.

Meanwhile, as shown in Fig. 10, by increasing the dispersion from 80 ps/nm/km to 98 ps/nm/km the BER of U1 changes in a linear fashion from 10^{-42} to

10^{-16}. However, this is irrelevant with the U2 and U3 as the proposed technique will increase the BER for both users. This shows that the U1 is dependent on the impairment from dispersion since its decision-making involves S1 and S2 only.

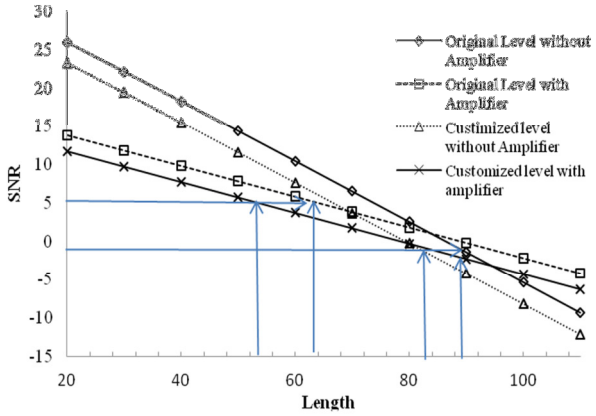

Fig. 9: SNR over fiber length

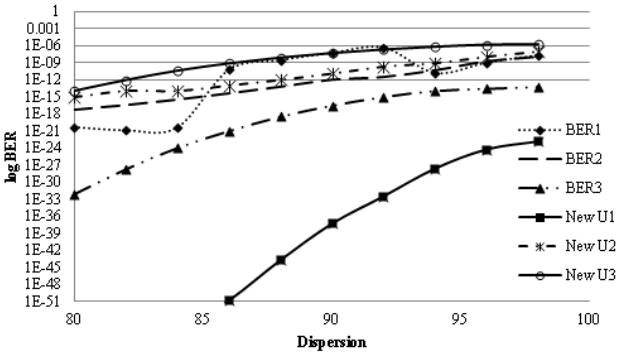

Fig. 10: log BER versus dispersion

5 Conclusion

We have proposed and developed a novel method to improve the performance of the DCDM system. Utilizing the signal processing methods and customisation of the signal level at the transmitter side, 7 dB improvements in comparison to the conventional DCDM system was achieved. In addition to that, and as opposed to the previously reported work, all channels show almost the same performance

References:

[1] E.S Hassan, "Performance Enhancement of Continuous-Phase Modulation Based OFDM Systems Using Chaotic Interleaving" *WSEAS transactions on systems*. vol. 12, 2013

[2] A. Rudziński. "Effective Number of Samples and Pseudo-Random Nonlinear Distortions in Digital OFDM Coded Signal". *Circuits, Systems, and Signal Processing*. Vol. 33, 2014, pp. 197-209

[3] D. Sheela, C. Chellamuthu, "A Cost Effective Approach for WDM Network Protection under Critical Duct Constraints", *WSEAS Transactions on Communications*, vol.11, 2012

[4] G. A. Mahdiraji, A.F. Abas, A. Malekmohammadi, M. Mokhtar, "Duty-Cycle Division Multiplexing: Alternative for High Speed Optical Networks". *Japanese Journal of Applied Physics*. Vol. 48, 2009

[5] G. A. Mahdiraji, et al., "Duty-Cycle-Division-Multiplexing: Bit Error Rate Estimation and Performance Evaluation", *Optical Review*, vol. 16, 2009, pp. 422-425

[6] A. Malekmohammadi, G.A. Mahdiraji, M.K. Abdullah, A.F. Abas, M. Mokhtar, M. F. A. Rashid , "Absolute Polar Duty Cycle Division Multiplexing", *International Review of Electrical Engineering*, vol. 3, 2008, pp. 395-400

[7] A. Malekmohammadi, M.K. Abdullah, G.A. Mahdiraji, A.F. Abas, M. Mokhtar, "Analysis of return-to-zero-on-off-keying over absolute polar duty cycle division multiplexing in dispersive transmission medium", *IET optoelectronics*. Vol. 3, 2009, pp. 197-206

[8] A. Malekmohammadi, G.A. Mahdiraji, A. Abas, M.K. Abdullah, M. Mokhtar., "Effect of self-phase-modulation on dispersion compensated absolute polar duty cycle division multiplexing transmission", *IET Optoelectronics*, vol. 3, 2009, pp. 207-214

[9] S.T. Cundiff and A. M. Weiner, "Optical arbitrary waveform generation" *Nat Photon*. Vol. 4, 2010, pp. 760-768

[10] U. Erez and R. Zamir, "Noise prediction for channel coding with side information at the transmitter", *IEEE Transactions on Information Theory*, vol. 46, 2000

[11] H. Y. Choi, T. Tsuritani, and I. Morita, "BER-adaptive flexible-format transmitter for elastic optical networks". *Optics Express,* vol. 20, 2012, pp. 18652-18658

[12] T. Liu, et all, "Feedback channel capacity inspired optimum signal constellation design for high-speed optical transmission", *in Conf. Lasers and Electro-Optics*, *USA*, 2012

[13] C.J. Anderson and J.A. Lyle "Technique for evaluating system performance using Q in numerical simulations exhibiting inter symbol interference", *Electronics Letters*. Vol. 30, 1994, pp. 71-72

[14] G. Kaddoum, J. Anthony, P. Lawrance, C. Roviras, "Chaos Communication Performance", *Theory and Computation. Circuits, Systems, and Signal Processing,* vol. 30, 2011, pp. 185-208

[15] A. Malekmohammadi, M.K Abdullah, G. A Mahdiraji, A.F. Abas, M. Mokhtar, M. F. A Rasid, S.M. Basir, "Decision circuit and bit error rate estimation for absolute polar duty cycle division multiplexing" *International Review of Electrical Engineering,* vol. 3, 2008, pp. 592-599

[16] M.N. Derahman, M.K. Abdullah, N.K. Dimyati, and A. Malekmohammadi, "Symbol coding customization for BER reduction in Duty-cycle Division Multiplexing Systems*" in Conf. 18th International Conference on Communications (part of CSCC '14)*, July 17-21, 2014